

Effect of bulk liquid BOD concentration on activity and microbial community structure of a nitrifying, membrane-aerated biofilm

Leon S. Downing · Robert Nerenberg

Received: 3 July 2008 / Revised: 2 September 2008 / Accepted: 4 September 2008
© Springer-Verlag 2008

Abstract Membrane-aerated biofilms (MABs) are an effective means to achieve nitrification and denitrification of wastewater. In this research, microsensors, fluorescence in situ hybridization (FISH), and modeling were used to assess the impact of bulk liquid biological oxygen demand (BOD) concentrations on the activity and microbial community structure of nitrifying MABs. With 1 g m^{-3} BOD in the bulk liquid, the nitrification rate was $1.3 \text{ g N m}^{-2} \text{ day}^{-1}$, slightly lower than the $1.5 \text{ g N m}^{-2} \text{ day}^{-1}$ reported for no bulk liquid BOD. With bulk liquid BOD concentrations of 3 and 10 g m^{-3} , the rates decreased to 1 and $0.4 \text{ g N m}^{-2} \text{ day}^{-1}$, respectively. The percent denitrification increased from 20% to 100% when the BOD increased from 1 to 10 g m^{-3} BOD. FISH results indicated increasing abundance of heterotrophs with increasing bulk liquid BOD, consistent with the increased denitrification rates. Modeling was used to assess the effect of BOD on nitrification rates and to compare an MAB to a conventional biofilm. The model-predicted nitrification rates were consistent with the experimental results. Also, nitrification in the MAB was much less sensitive to BOD inhibition than the conventional biofilm. The MAB achieved concurrent nitrification and denitrification, whereas little denitrification occurred in the conventional biofilm.

Keywords Nitrification · Denitrification · Wastewater · BOD inhibition · Membrane-aerated biofilm reactor · Membrane biofilm reactor

Introduction

One of the major challenges in wastewater treatment is achieving effective nitrogen removal. Nitrogen removal requires nitrification, an aerobic process requiring long solid retention times (SRTs), and denitrification, an anoxic process requiring an electron donor. New technologies that can achieve both nitrification and denitrification, while maximizing the use of influent biological oxygen demand (BOD) for denitrification, are critical for improving current wastewater treatment capabilities.

Biofilm systems can provide increased SRTs while minimizing process footprint (Rittmann 1987); however, competition of heterotrophs and nitrifiers in biofilm systems limits nitrification rates (Fernandez-Polanco et al. 2000; LaPara et al. 2006; Nogueira et al. 2002; Okabe et al. 1996b; van Benthum et al. 1997). Fast-growing heterotrophs dominate the outer biofilm, where BOD concentrations are high, while slower-growing nitrifiers dominate the deep portions of the biofilm, where BOD concentrations are lower (Okabe et al. 1996b). This is unfavorable for nitrifying bacteria, resulting in lower nitrification rates. The effect is most pronounced at high bulk liquid BOD concentrations, where there is significant BOD diffusion into the biofilm (Fernandez-Polanco et al. 2000; Rittmann and Manem 1992; Wanner and Gujer 1985; Wanner and Reichert 1996).

Membrane-aerated biofilms (MABs) may provide a more advantageous environment for nitrification in the presence of BOD. MABs have been studied for wastewater

L. S. Downing · R. Nerenberg (✉)
Department of Civil Engineering and Geological Sciences,
University of Notre Dame,
156 Fitzpatrick Hall,
Notre Dame, IN 46556, USA
e-mail: Nerenberg.1@nd.edu

Present address:
L. S. Downing
Freese and Nichols, Inc.,
4055 International Plaza, Suite 200,
Fort Worth, TX 76109, USA

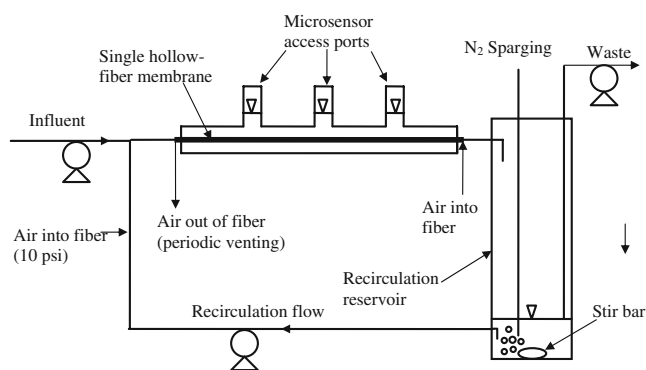
treatment in biofilm configurations (Hibiya et al. 2003; Satoh et al. 2004; Semmens et al. 2003; Walter et al. 2005) and hybrid (suspended and biofilm growth) configurations (Downing and Nerenberg 2007, 2008a). In MAB systems, air-supplying and biofilm-supporting membranes are placed in a nonaerated, well-mixed tank. MABs are counter-diffusion biofilms, and oxygen is highest deep in the biofilm, whereas BOD and ammonium are highest at the outer edge of the biofilm (Cole et al. 2004). Nitrifying bacteria grow in the deep, aerobic portions of the biofilm where BOD concentrations are low, and heterotrophic bacteria grow on the outer portions using nitrate or nitrite as electron acceptors (Cole et al. 2004; LaPara et al. 2006). LaPara et al. (2006) studied the impact of influent chemical oxygen demand, $\text{NH}_4^+\text{-N}$, and oxygen source (air or pure oxygen) on MABs. Both the organic loading rate and the carbon-to-nitrogen ratio (C to N) affected the abundance of ammonia-oxidizing bacteria (AOB), with high loading rates and high influent C to N resulting in little to no AOB.

The counter diffusion of BOD, ammonium, and oxygen also allows for nitrification and denitrification to occur in a single tank. When the bulk liquid is unaerated, high rates of denitrification can occur in the outer portion of the biofilm (Hibiya et al. 2003; Semmens et al. 2003; Terada et al. 2006) or in the suspended phase (Downing and Nerenberg 2008b). In membrane-aerated bioreactors (MABRs), where heterotrophs and nitrifiers are maintained in a biofilm with no suspended growth, nitrification is sensitive to the influent BOD concentration (Walter et al. 2005). At higher BOD loadings, a higher effluent BOD concentration exists in the bulk liquid, and BOD diffuses deeper in the biofilm, limiting nitrification (Rittmann and Manem 1992). In the hybrid membrane biofilm process (HMBP), heterotrophic bacteria are maintained in the bulk liquid, while nitrifying bacteria dominate in the MAB (Downing and Nerenberg 2007). In this system, the nitrification rate is insensitive to BOD loading but sensitive to the bulk liquid BOD concentration (Downing and Nerenberg 2008b).

While several studies have noted the inhibiting effect of BOD on nitrification and have observed the microbial community structure of MABs, there has been no systematic and quantitative study of inhibition for a range of BOD concentrations, nor a detailed examination of the effects of BOD on the microbial community structure and activity. Also, there has not been a quantitative comparison of MABs with conventional biofilms. This research reports on the impact of bulk liquid BOD concentrations on biofilm activity (nitrification and denitrification rates) and the microbial community structure of a nitrifying MAB. A combination of laboratory and modeling experiments were utilized to examine the impacts of BOD concentration on a nitrifying MAB. Modeling was also used to compare the impact of bulk liquid BOD concentration on an MAB and conventional biofilm.

Material and methods

Reactor configuration A reactor with a single hollow-fiber membrane was used to simulate an HMBP or MABR biofilm achieving total nitrogen (TN) removal (Fig. 1). This reactor was identical to the system previously used to study nitrite accumulation in an MAB (Downing and Nerenberg 2008a). The membranes were made from composite, microporous polyethylene with a dense, polyurethane core (HFM200TL, Mitsubishi Rayon, Japan). The reactor consisted of a hydraulic loop formed by two, 6-mm inside diameter glass tubes, each 20 cm in length. The glass tubes were connected to a peristaltic recirculation pump on one end and to a glass recirculation reservoir on the other (Fig. 1). The upper glass tube contained a single hollow-fiber membrane and had three 3-mm-diameter access ports. The ports were used for microsensor measurements of dissolved oxygen (DO), ammonium, nitrite, and nitrate in the biofilm. The recycle reservoir was continuously purged with nitrogen gas to maintain an anoxic bulk liquid, and a magnetic stir bar kept the reservoir well-mixed with a high shear velocity, minimizing biofilm growth on the glass surface. The total liquid volume in the reactor was 56 mL. A volume of 40 mL was maintained in the recirculation reservoir with an effluent pump. The influent flow rate was 2 mL min^{-1} , providing a hydraulic retention time (HRT) of 28 min. The short HRT prevented the accumulation of suspended nitrifying bacteria, and anoxic bulk liquid conditions during most of the experiments prevented nitrifying biofilms from growing on glass surfaces. The reactor temperature was approximately 22°C . The recircu-



Component	Inside Diameter	Length	Volume	Area
Glass Tube	6 mm	40 cm	5 mL	-
Rubber Tubing	6 mm	10 cm	1.25 mL	-
Reservoir	-	-	50 mL	-
Membrane	280 μm	18 cm	-	$2.7 \times 10^{-3} \text{ m}^2$

Fig. 1 Experimental setup, including a single hollow fiber membrane in a glass tube

lution flow rate was $50 \text{ cm}^3 \text{ min}^{-1}$, resulting in a fluid velocity of 30 cm s^{-1} and a Reynolds number of 680 inside the glass tube. The hollow-fiber membrane was normally operated in dead-end mode, but the fiber was vented on a daily basis to prevent accumulation of water condensate. Each column reactor was inoculated with activated sludge from the Platteville, WI municipal wastewater treatment plant, which was achieving nitrification to nitrate when the sludge was collected.

Testing conditions Three bulk liquid BOD conditions were tested on three different MABs. Influent ammonium was 3 g N m^{-3} , equivalent to a loading rate of $33 \text{ g N m}^{-2} \text{ day}^{-1}$. Both the ammonium and BOD loadings greatly exceeded the degradation rates of the MAB, so the influent concentrations were essentially equal to the effluent concentrations. The intramembrane pressure was 70 kPa in all experiments. The influent BOD concentrations were 1, 3, and 10 g m^{-3} in experiments 1, 2, and 3, respectively. Each test was conducted with a new membrane material and run for 56 days. Microsensor measurements were taken at days 42 and 56, and the membranes were sacrificed for fluorescence in situ hybridization (FISH) analysis on day 56.

Synthetic medium A minimal medium was used in these experiments. Distilled water was amended with $0.5 \text{ g NaH}_2\text{PO}_4 \cdot 7\text{H}_2\text{O}$ and aliquots of a calcium–iron and a trace mineral solution (Nerenberg and Rittmann 2002). An ammonium concentration of 3 g N m^{-3} was achieved by adding $(\text{NH}_4)_2\text{SO}_4$. Potassium acetate was added as a BOD source to achieve 1, 3, or 10 g BOD m^{-3} . This medium was designed to minimize interference with the microsensors used for microgradient measurements in the biofilm. The medium pH was approximately 7.0 and the temperature was approximately 22°C . The medium was maintained anoxic by sparging the medium with nitrogen gas and maintaining a positive pressure of nitrogen gas on the storage container.

Analytical methods Ammonia ($\text{NH}_3\text{-N}$) concentrations were monitored in the bulk liquid using the salicylate method (Hach, Loveland, CO, USA). A glass electrode pH meter was used to monitor pH. Nitrate ($\text{NO}_3^-\text{-N}$) and nitrite ($\text{NO}_2^-\text{-N}$) were analyzed by ion chromatography (ICS2500 with AS11/AG11 column and guard column, Dionex Corp, Sunnyvale, CA, USA).

Microsensor studies Clark-type oxygen microelectrodes (Revsbech and Jorgensen 1986) with a tip diameter of $10 \mu\text{m}$ were used to measure DO concentrations in the biofilms (Ox10, Unisense A/S, Aarhus, Denmark). Liquid ion exchange (LIX) microsensors were constructed to measure ammonium, nitrate, and nitrite concentrations in

the biofilm. LIX construction was completed as previously described (Geiseke and De Beer 2004). Nitrate (De Beer and Sweerts 1989) and ammonium (De Beer and van den Heuvel 1988) microsensors were constructed with a tip diameter of 3 to $5 \mu\text{m}$, and the nitrite electrodes had a tip diameter of 10 to $15 \mu\text{m}$ (De Beer et al. 1997). All measurements were taken at spatial intervals of $20 \mu\text{m}$ through the biofilm. The sensors were positioned throughout the biofilm with a micromanipulator (Model MM33-2, Unisense A/S, Aarhus, Denmark).

Microprofile measurements were made at each of the three sampling ports in the reactor on days 42 and 56. Three to five microprofiles were taken for each port. The biofilm was relatively homogeneous along membrane length for a given experiment. A total of nine to 15 sets of profiles were analyzed for each reactor on each sampling date.

Substrate fluxes into and out of the biofilm were calculated from microprofile measurements across the diffusion boundary layer, as previously described (Downing and Nerenberg 2008a).

FISH studies After microelectrode measurements were completed on day 56, FISH studies were carried out as previously described (Downing and Nerenberg 2008a). Briefly, the membrane was removed from the reactor and fixed in freshly prepared paraformaldehyde and washed in phosphate-buffered saline. Membrane-bound biofilms were embedded and sectioned at -20°C (Schramm et al. 2000). Each section was $5 \mu\text{m}$ thick. Sections were dehydrated and dried, and four FISH probes were implemented: Nso190, which targets the majority of AOB (Mobarry et al. 1996); NIT3, which targets *Nitrobacter spp.*, one of the dominant nitrite-oxidizing bacteria (NOB) species (Wagner et al. 1996); NSR1156, which targets *Nitrospira spp.*, the other dominant NOB species (Schramm et al. 1998); and EUB338, which targets general bacteria (Amann et al. 1990). Probes, hybridization conditions, and washing conditions are as described previously (Mobarry et al. 1996; Wagner et al. 1996; Schramm et al. 1998; and Amann et al. 1990). Oligonucleotides were synthesized and fluorescently labeled with fluorochromes Cy3, Cy5, or fluorescein isothiocyanate by Operon Biotechnologies, Inc. (Huntsville, AL, USA). Bacteria that hybridized with EUB338, but not with the specific probes, were assumed to be heterotrophs. DAPI was used as a counterstain. Images were examined with an epifluorescence microscope (Nikon Eclipse 90i).

Quantification was accomplished using MetaMorph software as previously described (Downing and Nerenberg 2008a; Molecular Devices, Sunnyvale, CA, USA). The area of a single, dispersed cell hybridized with each of the probes was first determined. This area was then assigned as a single cell. Areas of cell clusters in the biofilm were then assigned

cell counts via the automated cell-count function in MetaMorph. A grid of 10-by-10 μm squares was applied to each image, and cell counts in each grid square were made. These grids were then assigned distances from the membrane surface. Thresholding was completed manually and verified with manual cell counts of dispersed cells. A total of ten images were analyzed for each probe at each condition.

Modeling A biofilm model was developed using AQUASIM 2.0 (Wanner and Reichert 1996) to predict MAB performance under a wide range of bulk liquid BOD concentrations. The model was similar to the model described by Downing and Nerenberg (2008a); however, it was modified to include heterotrophic growth and decay.

Four microbial populations were included: heterotrophic bacteria, AOB, *Nitrobacter* spp., and *Nitrospira* spp. The kinetic parameters used in the model, as well as a detailed description of the kinetic processes, process stoichiometry, and physical parameters used in the model are shown in “Appendix.” The AOB parameters were assumed to be for *Nitrosomonas eutropha*, as previous MAB studies have shown this lineage to be the dominant AOB (Schramm et al. 2000; Downing and Nerenberg 2008a). *Nitrobacter* spp. and *Nitrospira* spp. were modeled separately, as they have distinct kinetics (Downing and Nerenberg 2008a).

The DO at the membrane–biofilm interface was fixed as a parameter in the model. The DO concentration at the membrane–biofilm interface was taken from experimental results. The biofilm density was assumed to be constant through the biofilm. Biofilm density can vary with depth in an MAB containing both nitrifiers and heterotrophs (Shanahan et al. 2005); however, assuming a constant density is a common simplifying assumption made when modeling with AQUASIM (Downing and Nerenberg 2008a; Elenter et al. 2007; Shanahan and Semmens 2004).

Using modeling, nitrification and denitrification rates were compared for MAB and a conventional, codiffusion biofilm (CB). In the CB model, all parameters were the same as for the MAB, except, the bulk liquid DO was set at 5 g m^{-3} and no oxygen was delivered at the base of the biofilm. Nitrification rate was based on the flux of ammonium in the model, while denitrification was based on the change of inorganic nitrogen in the model (i.e., ammonium oxidized minus the effluent nitrate and nitrite).

Results

Microsensor results

Profiles for oxygen, ammonium, nitrite, and nitrate through the biofilm were determined using microsensors. Profiles

for experiments 1, 2, and 3 are shown in Fig. 2. The average biofilm thicknesses were 110, 120, and 380 μm , respectively. Nitrite was present in all three profiles, which is consistent with previous research (Downing and Nerenberg 2008a,b; Terada et al. 2006). Higher nitrate concentrations, relative to the nitrite concentrations, were observed

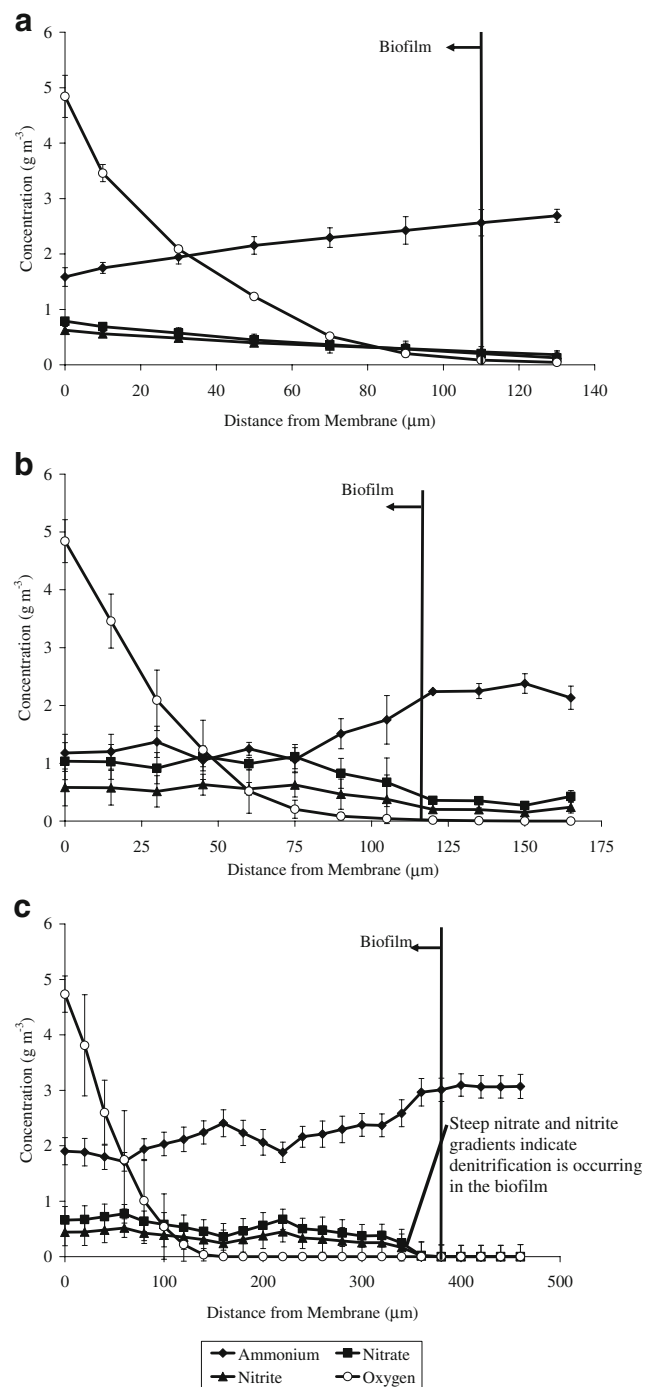


Fig. 2 Experimental profiles of ammonium, nitrite, nitrate, and oxygen in a membrane-aerated biofilm with a 1 g m^{-3} , b 3 g m^{-3} , and c 10 g m^{-3} BOD in the bulk liquid

in the biofilms exposed to higher bulk liquid BOD concentration. This was likely a result of the increased aerobic zone present in the biofilm exposed to higher bulk liquid BOD concentrations, where higher DO concentrations allow NOB to compete more effectively with AOB. In Fig. 2c, a significant decrease is observed in nitrate and nitrite at the beginning of the biofilm's anoxic zone. This suggests a significant amount of denitrification in this anoxic zone at higher bulk liquid BOD concentrations.

The rates of nitrification, nitrite production, and nitrate production were calculated from the microsensors profiles using the flux into or out of the biofilm (Fig. 3). With a bulk liquid BOD concentration of 1 g m^{-3} BOD, the nitrification rates was approximately $1.3 \text{ g N m}^{-2} \text{ day}^{-1}$, only slightly less than the $1.5 \text{ g N m}^{-2} \text{ day}^{-1}$ observed in a previous study with no added BOD (Downing and Nerenberg 2008a). Little to no denitrification was observed in both cases. When the bulk liquid BOD was 3 g m^{-3} , the nitrification rate decreased to $1 \text{ g N m}^{-2} \text{ day}^{-1}$, and it further decreased to $0.4 \text{ g N m}^{-2} \text{ day}^{-1}$ when the bulk liquid BOD was 10 g m^{-3} . This is most likely a result of the increased thickness of heterotrophic biomass, which leads to increased mass transfer resistance for ammonium. The degree of inhibition in our experiments was probably higher than a real wastewater, as the BOD was supplied as acetate, a readily degradable BOD source. Municipal wastewater would include a mixture of readily degradable and more slowly degradable BOD sources.

Denitrification in the biofilm increased with higher bulk liquid BOD concentrations. This was a result of increased diffusion of BOD into the biofilm. When the bulk liquid BOD concentration was 3 g m^{-3} , over 80% denitrification was achieved. Complete denitrification was achieved at 10 g m^{-3} BOD, although the nitrification rate was only 0.4 g N m^{-2}

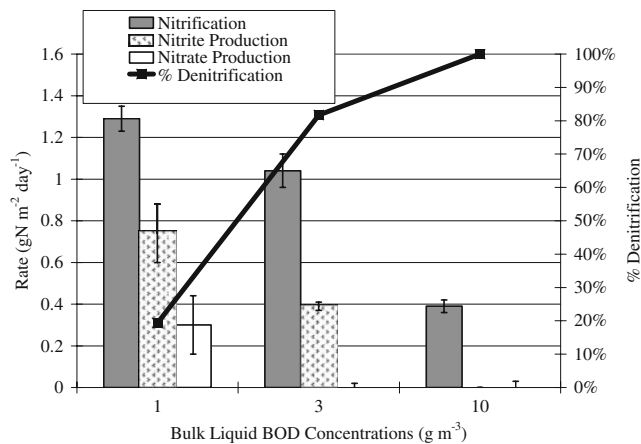


Fig. 3 Nitrification, nitrite production, nitrate production, and denitrification rates for the three experimental conditions tested. Denitrification is the difference between the nitrification rate and the nitrite and nitrate production rates of the biofilm

day^{-1} under this condition. When oxidized nitrogen was exported from the biofilm, it was mainly nitrite, which is consistent with shortcut nitrogen removal observed in previous MAB studies (Downing and Nerenberg 2008a,b; Hibiya et al. 2003; Schramm et al. 2000; Terada et al. 2006).

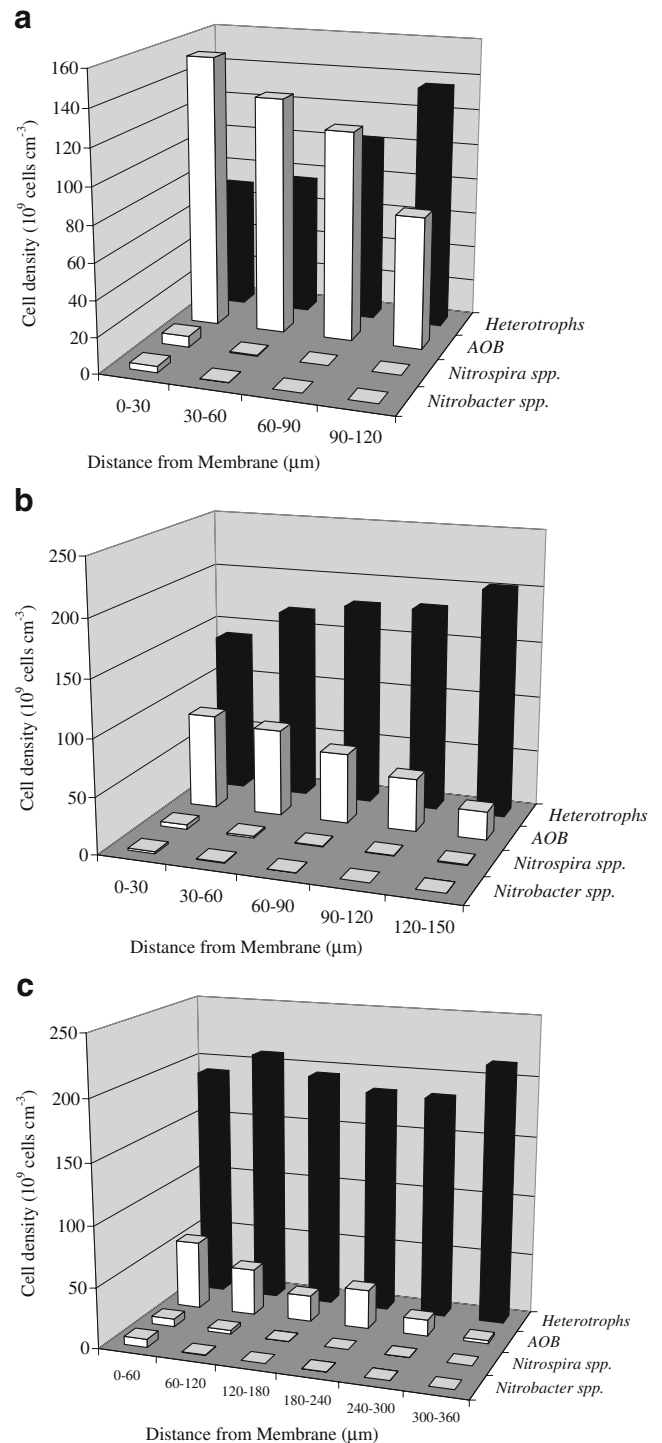


Fig. 4 Distribution of AOB, NOB, and heterotrophs through the membrane-aerated biofilm with **a** 1 g m^{-3} , **b** 3 g m^{-3} , and **c** 10 g m^{-3} BOD in the bulk liquid. Note the variation in the x-axis scale

FISH results

The distribution of AOB, NOB, and heterotrophs in the MABs was determined using FISH. As expected from the results described above, the AOB population densities decreased significantly with increasing bulk liquid BOD concentration (Fig. 4). In Fig. 4, “heterotrophs” are cells that hybridized with the universal probe but not the AOB or NOB probes. Heterotrophs dominated the outer biofilm in all three cases, which is similar to the stratification in nitrifying biofilms (Okabe et al. 1996a) and MABs (Cole et al. 2004; LaPara et al. 2006). Heterotrophs were present throughout the biofilm for all three bulk liquid BOD conditions, but the heterotrophs did not compose the majority of the biofilm until the bulk liquid BOD concentration reached 3 g m^{-3} .

The NOB populations showed a different trend than the AOB. At the low bulk liquid BOD concentrations, *Nitrospira* spp. was the dominant NOB and all of the NOB were mainly within $30 \mu\text{m}$ from the membrane surface. However, at a bulk liquid BOD concentration of 10 g m^{-3} , a larger aerobic zone existed in the biofilm. This larger aerobic zone may have favored *Nitrobacter* spp., which have a higher K_o value than *Nitrospira* spp. (Downing and Nerenberg 2008a). Overall, there was an increasing presence of NOB with increasing bulk liquid BOD concentration, which is consistent with the higher levels of nitrate in the biofilm at increased BOD concentrations. Note that error bars were omitted from Fig. 4 to simplify the presentation. Standard deviation for ten images ranged from 30% to 40% for the NOB densities. This large error is associated with the clustering of NOB within the biofilm, where portions of the biofilm effectively had no NOB, while others had elevated densities.

Modeling results

Comparison of model and experimental results The ammonium fluxes in the model and experiments were within 15% of each other (Table 1), and the nitrate and nitrite flux were generally in good agreement. The nitrate and nitrite concentrations at the outer edge of the biofilm were typically much lower than the ammonium concentration, making relative errors more significant. Based on the

accurate predictions for the three experimental conditions, it was assumed that the model was suitable for assessing the impact of BOD concentration on nitrification in MAB.

Following verification, the model was used to explore bulk liquid BOD concentrations ranging from 1 to 20 g m^{-3} (Fig. 5). Nitrification decreased drastically when BOD increased from 1 to 10 g m^{-3} , but the decrease in nitrification rate was less significant at higher BOD concentrations. Nitrite and nitrate were reduced within the biofilm at BOD concentrations above 3 g m^{-3} . Some nitrification occurred in the system even when the bulk liquid BOD concentration was as high as 20 g m^{-3} .

Comparison of CB and MAB The differences between an MAB and CB have been highlighted for a completely autotrophic nitrogen removal system (Lackner et al. 2008), but this is the first comparison of the differences between a heterotrophic–autotrophic MAB and conventional biofilm achieving TN removal. Based on modeling results, the nitrifying MAB had significantly higher nitrification rates than a CB, regardless of the bulk liquid BOD (Fig. 6). Some nitrification occurred in the MAB with effluent BOD concentrations as high as 20 g m^{-3} (Fig. 5), whereas no nitrification occurred in the CB with a bulk liquid BOD concentration of only 10 g m^{-3} .

Discussion

A combination of experimental and modeling results was used to assess the impact of bulk liquid BOD concentration on nitrification and denitrification in an MAB. Bulk liquid BOD, when supplied as acetate, slightly impacted nitrification at 1 g m^{-3} but had significant impacts at 3 and 10 g m^{-3} BOD. Heterotrophs increased in abundance with increasing bulk liquid BOD, forming a thicker heterotrophic layer that increased mass transfer resistance and decreased nitrification rates. Among nitrifying bacteria, AOB were more abundant than NOB, but NOB abundances increased at higher BOD concentrations.

Modeling was used to compare the effects of BOD on an MAB and a CB. In both an MAB and CB, nitrifiers are located in the interior of the biofilm, where the BOD

Table 1 Comparison of model-predicted and experimental fluxes into and out of the biofilm

Experiment	BOD concentration (g m^{-3})	Ammonium ($\text{g N m}^{-2} \text{ day}^{-1}$)		Flux nitrite ($\text{g N m}^{-2} \text{ day}^{-1}$)		Nitrate ($\text{g N m}^{-2} \text{ day}^{-1}$)	
		Exp	Model	Exp.	Model	Exp.	Model
1	1	-1.29	-1.45	0.74	1.04	0.30	0.35
2	3	-1.04	-0.97	0.19	0.07	0.07	0.04
3	10	-0.39	-0.45	0.00	0.00	0.00	0.00

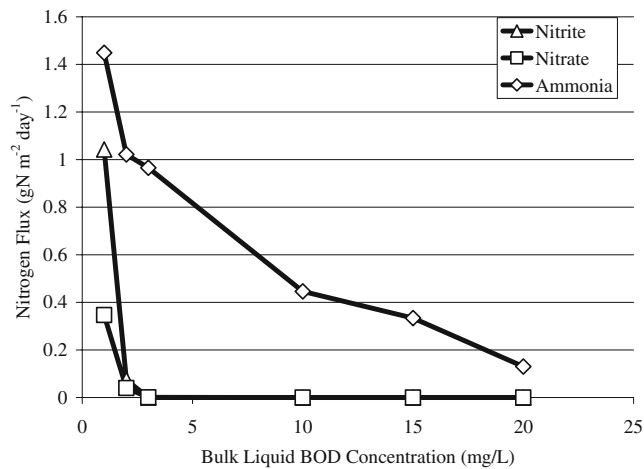


Fig. 5 Model-predicted impact of bulk liquid BOD concentration on nitrification, nitrite production, and nitrate production

concentration is low. However, in the MAB, the oxygen concentration is maximum in the interior of the biofilm, where the nitrifiers are located, as opposed to the exterior of the biofilm, where the heterotrophs dominate. This allows for a much higher nitrification rate in the MAB. Nitrite and nitrate are produced at the base of the biofilm in both MABs and CBs due to the location of nitrifying bacteria in both biofilms. However, in the MAB, the DO concentration decreases towards the outer edge of the biofilm, where higher BOD concentrations are present. This allows significant denitrification to occur. Denitrifi-

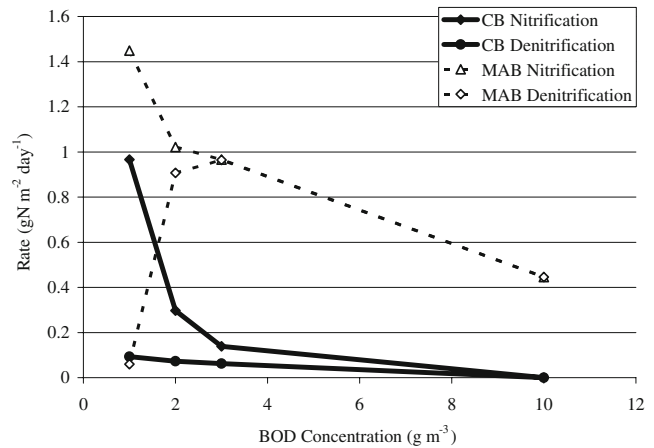


Fig. 6 Model-predicted nitrification and denitrification rates in a conventional biofilm (CB) and membrane-aerated biofilm (MAB) at different bulk liquid BOD concentrations

cation is limited in the CB, as oxygen and BOD are both high at the edge of the biofilm (Rittmann and Manem 1992; Wanner and Gujer 1985).

Our results suggest that MABs are well-suited for applications where concurrent nitrification and BOD oxidation is needed, such as nitrogen removal from wastewater. While nitrification rates decrease at higher BOD concentrations, MABs are less sensitive to BOD inhibition than CBs, and high denitrification rates can be achieved.

Appendix

Table 2 Kinetic parameters used for AOB and NOB

Var.	Description	Value	Reference
AOB			
$\hat{\mu}_{AOB}$	Maximum specific growth rate for AOB	0.48 day ⁻¹	Adapted from Prosser (1989)
Y_{AOB}	Yield for AOB	0.3 g X g NH ₄ ⁺ -N ⁻¹	Shanahan and Semmens (2004)
		g NH ₄ ⁺ -N g X ⁻¹	
\hat{q}_{AOB}	Maximum substrate utilization rate for AOB	1.6 day ⁻¹	Adapted from Prosser (1989)
b_{AOB}	Decay coefficient for NOB	0.13 day ⁻¹	Terada et al. (2006)
$K_{s,AOB}$	Half saturation coefficient for ammonium	0.9 g N m ⁻³	Shanahan and Semmens (2004)
$K_{o,AOB}$	Half saturation coefficient for oxygen	0.24 g N m ⁻³	Shanahan and Semmens (2004)
Nitrobacter spp.			
$\hat{\mu}_{Nit}$	Maximum specific growth rate for <i>Nitrobacter</i> spp.	0.31 day ⁻¹	Downing and Nerenberg (2008a, b)
Y_{Nit}	Yield for <i>Nitrobacter</i> spp.	0.08 g X g NO ₂ ⁻ -N ⁻¹	Downing and Nerenberg (2008a, b)
		g NO ₂ ⁻ -N g X ⁻¹	
\hat{q}_{NIT}	Maximum substrate utilization rate for <i>Nitrobacter</i> spp.	3.87 day ⁻¹	Adapted from Prosser (1989)
b_{Nit}	Decay coefficient for <i>Nitrobacter</i> spp.	0.1 day ⁻¹	Terada et al. (2006)
K_{s-Nit}	Half saturation coefficient for nitrite	0.39 g N m ⁻³	Downing and Nerenberg (2008a, b)
K_{o-Nit}	Half saturation coefficient for oxygen	0.51 g N m ⁻³	Downing and Nerenberg (2008a, b)
Nitrospira spp.			
$\hat{\mu}_{Nsr}$	Maximum specific growth rate for <i>Nitrospira</i> spp.	0.28 day ⁻¹	Downing and Nerenberg (2008a, b)
Y_{Nsr}	Yield for <i>Nitrospira</i> spp.	0.15 g X g NO ₂ ⁻ -N ⁻¹	Downing and Nerenberg (2008a, b)

Table 2 (continued)

Var.	Description	Value	Reference
\hat{q}_{NSR}	Maximum substrate utilization rate for <i>Nitospira</i> spp.	1.87	Adapted from Prosser (1989)
b_{Nsr}	Decay coefficient for <i>Nitospira</i> spp.	0.1	Terada et al. (2006)
K_{s-Nsr}	Half saturation coefficient for nitrite	0.27	Downing and Nerenberg (2008a, b)
K_{o-Nsr}	Half saturation coefficient for oxygen	0.4	Downing and Nerenberg (2008a, b)

X is biomass expressed as dry weight

Table 3 Kinetic parameters used for heterotrophic bacteria

Var.	Description	Value	Reference
\hat{q}_{BOD}	Maximum specific growth rate for heterotrophs	6.2	Weissmann (1997)
$Y_{BOD,O}$	Aerobic yield for heterotrophs	0.4	Shanahan and Semmens (2004)
$Y_{BOD,NO}$	Anoxic yield for heterotrophs	0.4	Weissmann (1997)
\hat{q}_{BOD}	Maximum substrate utilization rate for heterotrophs	10	Adapted from Prosser (1989)
b_{Bod}	Decay coefficient for Heterotrophs	0.13	Terada et al. (2006)
$K_{s,BOD}$	Half saturation coefficient for BOD	0.9	Shanahan and Semmens (2004)
$K_{o,BOD}$	Half saturation coefficient for oxygen	0.24	Shanahan and Semmens (2004)
$K_{nitrite,BOD}$	Half saturation coefficient for nitrite	0.24	Shanahan and Semmens (2004)
$K_{nitrate,BOD}$	Half saturation coefficient for nitrate	0.24	Shanahan and Semmens (2004)

Table 4 Physical parameters used in the membrane aerated biofilm model

Par.	Description	Value	Reference
ρ	Biofilm density	10	Rittmann and McCarty (2001)
$D_{NH_4^+-N}$	Diffusivity of ammonium	1.5×10^{-4}	Adapted from Schramm et al. (1999)
D_{NO_2-N}	Diffusivity of nitrite	1.4×10^{-4}	Adapted from Schramm et al. (1999)
D_{NO_3-N}	Diffusivity of nitrate	1.4×10^{-4}	Adapted from Schramm et al. (1999)
D_{O_2}	Diffusivity of oxygen	1.5×10^{-4}	Adapted from Schramm et al. (1999)
D_{BOD}	Diffusivity of BOD	8.23×10^{-5}	Shanahan and Semmens (2004)
LDL	Thickness of liquid diffusion layer	7	Calculated for this study

Table 5 Kinetic rate expressions

Process	Rate expression
Aerobic ammonium oxidation	$\hat{q}_{AOB} Y_{AOB} \frac{NH_4^+}{NH_4^+ + K_{s,AOB}} \frac{O_2}{O_2 + K_{o,AOB}} X_{AOB}$
Aerobic nitrite oxidation, <i>Nitrobacter</i> spp.	$\hat{q}_{Nit} Y_{Nit} \frac{NO_2}{NO_2 + K_{s,Nit}} \frac{O_2}{O_2 + K_{o,Nit}} X_{Nit}$
Aerobic nitrite oxidation, <i>Nitospira</i> spp.	$\hat{q}_{Nsr} Y_{Nsr} \frac{NO_2}{NO_2 + K_{s,Nsr}} \frac{O_2}{O_2 + K_{o,Nsr}} X_{Nsr}$
Aerobic BOD oxidation	$\hat{q}_{BOD} Y_{BOD} \frac{BOD}{BOD + K_{s,BOD}} \frac{O_2}{O_2 + K_{o,BOD}} X_{BOD}$
Anoxic BOD oxidation, nitrate	$\hat{q}_{BOD} Y_{BOD} \frac{BOD}{BOD + K_{s,BOD}} \frac{NO_3^-}{NO_3^- + K_{nitrate,BOD}} X_{BOD} \frac{K_{o,BOD}}{K_{o,BOD} + O_2}$
Anoxic BOD oxidation, nitrite	$\hat{q}_{BOD} Y_{BOD} \frac{BOD}{BOD + K_{s,BOD}} \frac{NO_2^-}{NO_2^- + K_{nitrite,BOD}} X_{BOD} \frac{K_{o,BOD}}{K_{o,BOD} + O_2}$
Decay of heterotrophs	$b_{BOD} \times X_{BOD}$
Decay of AOB	$b_{AOB} \times X_{AOB}$
Decay of <i>Nitrobacter</i> spp.	$b_{Nit} \times X_{Nit}$
Decay of <i>Nitospira</i> spp.	$b_{Nsr} \times X_{Nsr}$

Table 6 Stoichiometric matrix

	BOD	NH ₄ ⁺ -N	NO ₂ ⁻ -N	NO ₃ ⁻ -N	O ₂	X _{AOB}	X _{Nit}	X _{Nsr}	X _{het}
Aerobic ammonium oxidation	–	$-\frac{1}{Y_{het,O}}$	$\frac{1}{Y_{AOB}}$	–	$-\frac{(3.42-1.42 \times Y_{AOB})}{Y_{AOB}}$	1	–	–	–
Aerobic nitrite oxidation, <i>Nitrobacter</i> spp.	–	–	$-\frac{1}{Y_{Nit}}$	$\frac{1}{Y_{Nit}}$	$-\frac{(1.14-1.42 \times Y_{Nit})}{Y_{Nit}}$	–	1	–	–
Aerobic nitrite oxidation, <i>Nitrospira</i> spp.	–	–	$-\frac{1}{Y_{Nsr}}$	$\frac{1}{Y_{Nsr}}$	$-\frac{(1.14-1.42 \times Y_{Nsr})}{Y_{Nsr}}$	–	–	1	–
Aerobic BOD oxidation	$-\frac{1}{Y_{het,O}}$	–	–	–	$-\frac{(1-1.42 \times Y_{BOD,O})}{Y_{BOD,O}}$	–	–	–	1
Anoxic BOD oxidation, NO ₃ ⁻	$-\frac{1}{Y_{het,NO}}$	–	–	$-\frac{(5.81-4.06 \times Y_{BOD,NO})}{Y_{BOD,NO}}$	–	–	–	–	1
Anoxic BOD oxidation, NO ₂ ⁻	$-\frac{1}{Y_{het,NO}}$	–	$-\frac{(1.71-1.52 \times Y_{BOD,NO})}{Y_{BOD,NO}}$	–	–	–	–	–	1
Decay of Het.	–	–	–	–	–	–	–	–	–1
Decay of AOB	–	–	–	–	–	–1	–	–	–
Decay of <i>Nitrobacter</i> spp.	–	–	–	–	–	–	–1	–	–
Decay of <i>Nitrospira</i> spp.	–	–	–	–	–	–	–	–1	–

References

- Amann R, Krumholz L, Stahl D (1990) Fluorescent-oligonucleotide probing of whole cells for determinative, phylogenetic, and environmental studies in microbiology. *J Bacteriol* 172:762–770
- Cole AC, Semmens MJ, LaPara TM (2004) Stratification of activity and bacterial community structure in biofilms grown on membranes transferring oxygen. *Appl Environ Microbiol* 70(4):1982–1989
- De Beer D, Sweerts J-PRA (1989) Measurement of nitrate gradients with an ion-selective microelectrode. *Anal Chim Acta* 219:351–356
- De Beer D, van den Heuvel JC (1988) Response of ammonium-selective microelectrodes based on the neutral carrier nonactin. *Talanta* 35(9):728–730
- De Beer D, Schramm A, Santegoeds C, Kuhl M (1997) A nitrite microsensor for profiling environmental biofilms. *Appl Environ Microbiol* 63(3):973–977
- Downing L, Nerenberg R (2007) Microbial ecology and performance of a hybrid membrane biofilm process for concurrent nitrification and denitrification. *Water Sci Technol* 55(8–9):355–362
- Downing L, Nerenberg R (2008a) Effect of oxygen gradients on performance and microbial community structure of a nitrifying, membrane-aerated biofilm. *Biotechnol Bioeng*. doi:10.1002/bit.22018
- Downing L, Nerenberg R (2008b) Total nitrogen removal in a hybrid, membrane-aerated activated sludge process. *Water Res* 42(14):2403–2410. doi:10.1016/j.watres.2008.06.006
- Elenter D, Milferstedt K, Zhang W, Hausner M, Morgenroth E (2007) Influence of detachment on substrate removal and microbial ecology in a heterotrophic/autotrophic biofilm. *Water Res* 41:4657–4671
- Fernandez-Polanco F, Mendez E, Uruena MA, Villaverde S, Garcia PA (2000) Spatial distribution of heterotrophs and nitrifiers in a submerged biofilter for nitrification. *Water Res* 34(16):4081–4089
- Geiseke A, De Beer D (2004) Use of microelectrodes to measure in situ microbial activities in biofilms, sediments, and microbial mats. In: Kowalchuk G, de Bruijn F, Head I, Akkermans A, van Elsas J (eds) *Molecular microbial ecology manual*. 2nd edn. Springer, Heidelberg
- Hibiya K, Terada A, Tsuneda S, Hirata A (2003) Simultaneous nitrification and denitrification by controlling vertical and horizontal microenvironment in a membrane-aerated biofilm reactor. *J Biotechnol* 100(1):23–32
- Lackner S, Terada A, Smets BF (2008) Heterotrophic activity compromises autotrophic nitrogen removal in membrane-aerated biofilms: results of a modeling study. *Water Res* 42(4–5):1102–1112
- LaPara TM, Cole AC, Shanahan JW, Semmens MJ (2006) The effects of organic carbon, ammoniaical-nitrogen, and oxygen partial pressure of the stratification of membrane-aerated biofilms. *J Ind Microbiol Biotech* 33(4):315–323
- Mobarry BK, Wagner M, Urbain V, Rittmann BE, Stahl DA (1996) Phylogenetic probes for analyzing abundance and spatial organization of nitrifying bacteria. *Appl Environ Microbiol* 62(6):2156–2162
- Nerenberg R, Rittmann B (2002) Perchlorate reduction in a hydrogen-based membrane-biofilm reactor. *J AWWA* 95(2):10
- Nogueira R, Melo LF, Purkhold U, Wuertz S, Wagner M (2002) Nitrifying and heterotrophic population dynamics in biofilm reactors: effects of hydraulic retention time and the presence of organic carbon. *Water Res* 36(2):469–481
- Okabe S, Hiratia K, Ozawa Y, Watanabe Y (1996a) Spatial microbial distributions of nitrifiers and heterotrophs in mixed-population biofilms. *Biotechnol Bioeng* 50(1):24–35
- Okabe S, Oozawa Y, Hirata K, Watanabe Y (1996b) Relationship between population dynamics of nitrifiers in biofilms and reactor performance at various C:N ratios. *Water Res* 30(7):1563–1572
- Prosser JI (1989) Autotrophic nitrification in bacteria. *Adv Microb Physiol* 30:125–181
- Revsbech NP, Jorgensen BB (1986) Microelectrodes: their use in microbial ecology. *Adv Microbiol Ecol* 9:293–352
- Rittmann BE (1987) Aerobic biological treatment. *Environ Sci Technol* 21(2):128–135
- Rittmann BE, Manem JA (1992) Development and experimental evaluation of a steady-state, multispecies biofilm model. *Biotechnol Bioeng* 39(9):914–922
- Rittmann BE, McCarty PL (2001) *Environmental biotechnology: Principles and applications*. McGraw Hill, New York, New York
- Satoh H, Ono, H, Rulin B, Kamo J, Okabe S, Fukushi K-I (2004) Macroscale and microscale analyses of nitrification and denitri-

- fication in biofilms attached on membrane aerated biofilm reactors. *Water Res* 38(6):1633–1641
- Schramm A, DeBeer D, Wagner M, Amann R (1998) Identification and activities in situ of *Nitrosospira* and *Nitrospira* spp. as dominant populations in a nitrifying fluidized bed reactor. *Appl Environ Microbiol* 64(9):3480–3485
- Schramm A, De Beer D, van den Heuvel JC, Ottengraf S, Amann R (1999) Microscale distribution of populations and activities of *Nitrosospira* and *Nitrospira* spp. along a macroscale gradient in a nitrifying bioreactor: quantification by in situ hybridization and the use of microsensors. *Appl Environ Microb* 65(8):3690–3696
- Schramm A, De Beer D, Gieseke A, Amann R (2000) Microenvironments and distribution of nitrifying bacteria in a membrane-bound biofilm. *Environl Microbiol* 2(6):680–686
- Semmens MJ, Dahm K, Shanahan J, Christianson A (2003) COD and nitrogen removal by biofilms growing on gas permeable membranes. *Water Res* 37(18):4343–4350
- Shanahan J, Semmens MJ (2004) Multipopulation model of membrane-aerated biofilms. *Environ Sci Technol* 38(11):3176–3183
- Shanahan J, Cole AC, Semmens MJ, LaPara TM (2005) Acetate and ammonium diffusivity in membrane-aerated biofilms: improving model predictions using experimental results. *Water Sci Technol* 52(7):121–126
- Terada A, Yamamoto T, Igarashi R, Tsuneda S, Hirata A (2006) Feasibility of a membrane-aerated biofilm reactor to achieve controllable nitrification. *Biochem Eng J* 28(2):123–130
- van Benthum WAJ, van Loosdrecht MCM, Heijnen JJ (1997) Control of heterotrophic layer formation on nitrifying biofilms in a biofilm airlift suspension reactor. *Biotechnol Bioeng* 53(4):397–405
- Wagner M, Rath G, Koops HP, Flood J, Amann R (1996) In situ analysis of nitrifying bacteria in sewage treatment plants. *Water Sci Technol* 34:237–244
- Walter B, Haase C, Rabiger N (2005) Combined nitrification/denitrification in a membrane reactor. *Water Res* 39(13):2781–2788
- Wanner O, Gujer W (1985) Competition in biofilms. *Water Sci Technol* 17(2–3):27–44
- Wanner O, Reichert P (1996) Mathematical modeling of mixed-culture biofilms. *Biotechnol Bioeng* 49(2):172–184
- Weismann U (1997) Biological nitrogen removal from wastewater. In: Fiechter A (ed) *Advances in biochemical engineering/biotechnology*. Springer-Verlag, Berlin, pp 113–154